

Juno Microwave Radiometer Patch Array Antennas

N. Chamberlain, J. Chen, P. Focardi, R. Hodges, R. Hughes, J. Jakoboski,
J. Venkatesan, M. Zawadzki
Jet Propulsion Laboratory, California Institute of Technology.
E-mail: Neil.F.Chamberlain@jpl.nasa.gov

Introduction

Juno is a mission in the NASA New Frontiers Program with the goal of significantly improving our understanding of the formation and structure of Jupiter [1]. One of the instruments in the Juno payload is a six-frequency microwave radiometer (MWR) comprising six receivers, each of which is fed by a separate antenna. Patch arrays are used for the two lowest frequencies (0.6 GHz and 1.25 GHz), slot arrays are used for the middle three frequencies (2.6 GHz, 5.2 GHz, and 10 GHz), and a corrugated horn is used for the highest frequency (22 GHz). The different antenna configurations were chosen based on a variety of requirements, including pattern and sidelobe performance, loss, on-orbit environmental conditions, mass, and volume. This paper discusses the modeling and measurement of the two patch array antennas, which are termed A1 and A2 respectively. An overview of the antenna architecture, design, and development at JPL is provided, along with estimates of performance and the results of measurements.

Antenna Design and Construction

Patch arrays were selected for the lowest frequencies of the MWR instrument primarily because they can meet the pattern, sidelobe, and loss requirements within an acceptable mass and volume footprint. A summary of design requirements is given in Table 1. The patch arrays for 0.6 GHz and 1.25 GHz are essentially frequency-scaled versions of each other, so a common approach to design, modeling, fabrication, and test can be used.

Table 1. Design Requirements

Description	Unit	A1	A2
Center frequency	MHz	600	1250
Bandwidth	%	≥ 4.5	
Beamwidth (3dB)	deg	≤ 22	
Sidelobe levels			
$25^\circ < \theta \leq 32^\circ$	dB	≤ -24	
$32^\circ < \theta \leq 40^\circ$	dB	≤ -28	≤ -27
$40^\circ < \theta \leq 70^\circ$	dB	≤ -35	≤ -34
$70^\circ < \theta \leq 100^\circ$	dB	≤ -43	≤ -42
$100^\circ < \theta \leq 150^\circ$	dB	≤ -45	
Avg. Return Loss	dB	≥ 15	
Insertion Loss	dB	≤ 1.65	≤ 1.75
Polarization	-	linear	
Pointing Accuracy	mrad	≤ 9	
Temperature	°C	-135 to +120	
Vibration	grms	40.6	23.5
Mass	(kg)	14	5

The array aperture consists of 25 patch elements in a 5-by-5 square grid with >0.5 wavelength element spacing. The patch elements are probe fed through a corporate feed network of power dividers and coaxial cables (Fig. 1). The radiating elements are attached to the top (groundplane) side of an aluminum honeycomb panel, while the feed network is attached to the bottom side. Coaxial feed-throughs connect the patch elements to the feed network. The power dividers are fabricated using air-stripline Wilkinson circuits and quarter-wavelength impedance transformers that produce a 5-way unequal

power split. The design is identical for each circuit. The feed network approximates a separable Taylor distribution with -30dB sidelobes. The sidelobe levels in Table 1 are integrated over phi and the defined ranges of theta. The resulting pattern taper minimizes synchrotron radiation from Jupiter.

The antenna element is a single layer patch on a rectangular block of dielectric honeycomb. The patch height and low permittivity substrate result in an element bandwidth of about 9%, as defined by a minimum return loss of 10dB and an average return loss over the band of 15dB or better.

The patch is fabricated from carbon-graphite co-cured with aluminum foil on both sides to reduce mass and provide low coefficient of thermal expansion (CTE). The patch, dielectric honeycomb substrate, and Aluminum honeycomb panel are bonded together with film adhesive.

There is a grounding wire at the center of the patch to aid in discharging static, and the substrate and bonding adhesives are carbon-loaded to further aid static discharge (the electron flux density on Jovian orbit is sufficiently high that electrons will penetrate the patch and eventually will accumulate in the substrate).

Figure 1. Array configuration and feed network.

Carbon-loading of adhesives and pre-pregs is a particularly troublesome expedient because performance is a somewhat sensitive function of the degree of added carbon powder. The key electrical performance metrics in this application are: a) sufficiently low resistivity to facilitate static discharge, and b) sufficiently high resistivity to limit skin effect losses. Furthermore, addition of carbon black to adhesives tends to reduce strength, especially at temperature extremes. JPL conducted an extensive program of qualification and testing to determine the optimal percentage of carbon loading.

The coaxial cables in the power divider network have a dielectric of silicon-dioxide that results in low insertion loss (0.4dB/m at 1.25GHz) and a very stable phase change with respect to temperature (<0.2 degree/ft between ±100C at 1.25GHz). The silicon dioxide dielectric also has better resilience to the Jovian radiation environment compared to typical coaxial cable dielectrics, such as Teflon. The cables are phase matched to within ±2° (measured to be typically within 0.6°) to provide a feed distribution with uniform phase. The cable connecting to the center of each power divider is 90 degrees longer than the others to make up for the fact that the stripline circuit from that port does not have a quarter wavelength impedance transformer. This was done to simplify the circuit board and minimize the footprint of the power divider housing (the power divider circuit assembly fits between the rows of connectors, making the cable routing easier).

The power divider assembly is shown in Fig. 2. The stripline circuit is printed on a thin Duroid circuit board. The board is held between two halves of machined aluminum

housing but is free to move about its center to accommodate differences in CTEs in the housing and board. The housing is fastened using nuts and screws.

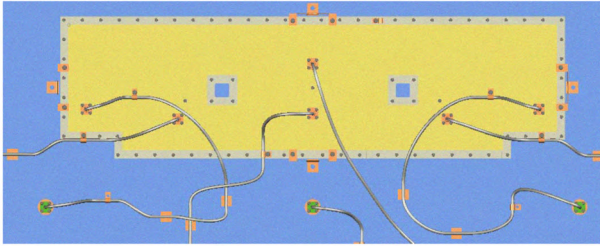


Figure 2. Power divider assembly.

A 3.5mm coaxial jack attaches to a boss milled into the housing. A tinned copper stress-relief ribbon is soldered to the pin and circuit board at each interconnect. Surface-mount isolation resistors are also soldered to the circuit board. It is important to have

good continuity of return currents through the coaxial sleeve at the transition. To this end, the housing is designed with a Keensert that allows the top-half and bottom half of this sleeve to be clamped together at the interconnect. The mass of each A1 power divider assembly, including all mounting hardware, is less than 0.5kg.

Electrical Design Procedure and Modeling

The Juno spacecraft is hexagonal in cross-section, with A1 taking up one entire face. The other 5 antennas are co-located on a different face. Array configuration and feed distribution for A1 were first estimated using an array factor code. Next, bandwidth, sidelobe, and pattern performance were calculated using a moment method model (Ansoft Designer) of the aperture, assuming ideal excitations from the power divider network. A scale model (at Ku band) of A1 was built in order to assess potential interactions with spacecraft structures; notably solar panels that protrude slightly into the field of view of A1 (these panels had a negligible effect on pattern performance). The aperture model was also constructed in HFSS, which produced good agreement with the moment method results.

The power divider circuit board was first designed using a moment method code (Ansoft Designer). The design was then transferred to an HFSS model to include details of the housing and interconnect. A network model of the entire feed network was constructed in Ansoft Designer. The model consists of synthesized (and later measured) S-parameters of the power divider, and models for the coaxial cables that include insertion loss, insertion phase, and impedance variations. The network model of the feed and HFSS model of the aperture were dynamically linked to facilitate co-simulation. The procedure for designing A2 followed the procedure for A1, the two antennas being frequency scaled versions of each other.

Performance and Measurements

The Juno A1 and A2 MWR patch array antennas were measured in a spherical near field antenna range at Nearfield Systems Inc. Measured antenna patterns are compared with predicted antenna patterns in Fig. 3. There is generally good agreement between the measured and modeled antenna patterns for these antennas, with A1 yielding better agreement than A2. Agreement is better for A1 (particularly in the back half space) because its larger aperture is blocked less by the antenna support structure in the measurement facility. In terms of integrated total field patterns, the agreement between measured patterns and modeled antenna patterns is typically 50dB or better, allowing for accurate prediction of antenna performance.

A summary of directivity, gain, insertion loss, and return loss is given in Table 2. Gain was computed using standard gain horns and the substitution method. The accuracy of the gain measurement at the A1 and A2 frequencies is ± 0.3 dB. The gain measurement serves to verify (by bounding) the insertion loss calculation. Insertion loss was calculated from the network model using measured power divider and coaxial cable s-parameters. There is generally good agreement between loss measurements and loss calculations.

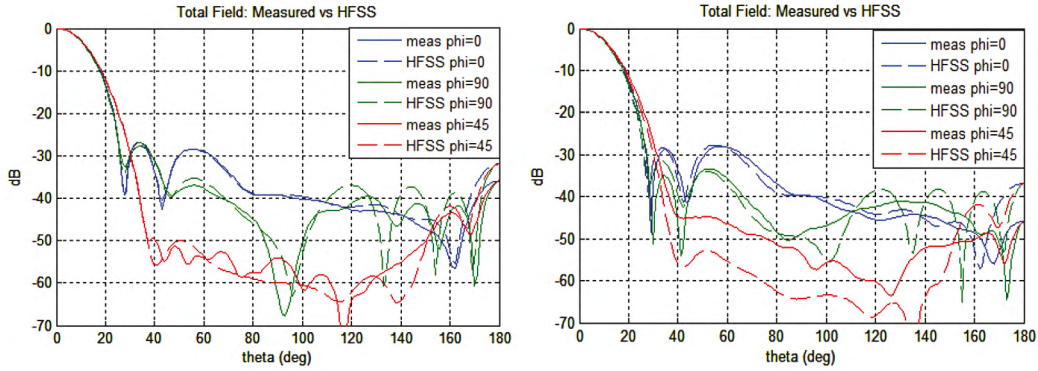


Figure 3: Measured versus modeled antenna patterns: A1 (left), A2 (right).

Table 2. Gain and loss measurements

	A1	A2
Computed directivity (dBi)	19.7	19.8
Measured gain (dBi)	18.6	18.9
Insertion loss from gain (dB)	1.1	0.9
Insertion loss from model (dB)	1.0	1.2
Average measured return loss (dB)	19.2	18.5
Average modeled return loss (dB)	18.6	21.9

Conclusions

The requirements, design, and performance of the Juno Microwave Radiometer patch array antennas were discussed. The antennas meet both the electrical performance and environmental requirements. There is generally good agreement between measurements and calculations.

References

- [1] P. Pingree et al, “Microwave Radiometers from 0.6 to 22 GHz for Juno, A Polar Orbiter around Jupiter”, IEEE Aerospace Conference, Big Sky, MT, 2008.

Acknowledgements

The research described in this paper was carried out at the Jet Propulsion Laboratory, California Institute of Technology, under a contract with the National Aeronautics and Space Administration. Reference herein to any specific commercial product, process, or service by trade name, trademark, manufacturer, or otherwise, does not constitute or imply its endorsement by the United States Government or the Jet Propulsion Laboratory, California Institute of Technology.